International Journal of Science and Research (IJSR)
ISSN: 2319-7064
Impact Factor 2024: 7.101

A Numerical Analysis of Non-Newtonian Power-Law Fluid Flow in a Lid-Driven Cavity with Variable Lid Motion

Mayank K Patel[1], Dr. Mohini B. Desai[2]

[1]Department of Mathematics, Shree Swaminarayan Science College, Swaminarayan University, Kalol, Gujrat, India
Email: *mk.mitha1995[at]gmail.com*

[2]Department of Mathematics, Shree Swaminarayan Science College, Swaminarayan University, Kalol, Gujrat, India
Email: *mohinidesai1218[at]swaminarayanuniversity.ac.in*

Abstract: ***The Numerical Study of flow behaviour in a two- dimensional square lid- driven cavity containing power- law fluids. The work aims to investigate the influence of the variation of the moving length of the top lid on the fluid flow behaviour, velocity profiles and vortex creation. The power- law fluid model is employed to simulate non- Newtonian fluids with power-law indices varying from shear- thinning*** $(\boldsymbol{n < 1})$ ***to shear- thickening*** $(\boldsymbol{n > 1})$ ***fluids. The finite volume method with a staggered grid arrangement and the simple algorithm for the pressure- velocity coupling technique is employed to solve the governing equations. The results show that a decrease in the moving length of the top lid results in localized flow perturbations with substantial influences on the primary vortex intensity and secondary vortex formation. The flow penetration inside the cavity is deeper for shear- thinning fluids with a smaller moving length, while resistance to flow is higher for shear- thickening fluids. The Reynolds number is held constant at*** $\boldsymbol{Re = 100}$ ***for all computations to demonstrate the dominance of viscous forces.***

Keywords: Lid-driven cavity, Power-law fluids, non-Newtonian flow, finite volume method, moving lid length

1. Introduction

The lid-driven cavity flow is a test problem in computational fluid dynamics (CFD), commonly employed as a benchmark for the validation of numerical solutions for incompressible viscous flows. In the standard problem, a square cavity with a moving top lid is considered, which causes recirculation inside the cavity. This problem has been widely investigated for Newtonian fluids [1,2], but there has been a growing interest in non-Newtonian fluids because of their importance in various industries like polymers, food and biomedical application.

Power-law fluids, also known as Ostwald-de Waele fluids, have viscosities that depend on the shear rate, given by the relation $\eta = K * Y^{n-1}$, where K is the consistency index, Y is the shear rate and n is the power-law index.

For $n = 1$, the fluid is Newtonian;
$n < 1$ indicates shear-thinning,
$n > 1$ indicates Shear-thickening behaviour.

Most studies on lid-driven cavities assume the entire top lid moves $[3 - 5]$. However, practical scenarios, such as partial agitation in mixers or localized shear in rheological devices, involve only a portion of the lid moving. This paper investigates the effect of varying moving lengths (L_m/L, where L is the cavity side length) of the top lid on the Power-law fluid flow. The moving lengths are taken as $0.25L, 0.50L, 0.75L,$ and $1.00L$ on the top lid. The simulations are carried out for $\mathrm{Re} = 100$, with n varying from 0.5 to 1.5.

The objectives are:

- To analyse the streamline patterns and vortex structures.
- To evaluate velocity profiles along cavity centrelines.
- To assess the impact of non-Newtonian index on flow behaviour under partial lid motion.

2. Numerical Method

Governing equations for fluid flow represent mathematical expressions of fundamental physical principles: conservation of mass (Continuity), momentum $(F = ma)$ and energy. These are commonly expressed as the Navier-Stokes equation, which can be in differential form for point-by-point analysis or integral form for a control volume.

The Governing equation for incompressible, steady, viscous, laminar and generalized non-Newtonian flow in the two-dimensional rectangular cavity.

1) Continuity Equation

$$\nabla_\alpha . (\rho u_\alpha) = 0 \qquad \ldots\ldots\ldots 1$$

This equation represents the conservation of mass.

For an incompressible fluid, the density (ρ) is constant, so the equation simplifies to the divergence of velocity being zero: $\nabla . u = 0$.

2) Momentum Equation

$$\nabla_{\beta\alpha} . (u_\alpha u_\beta) = -\nabla_\alpha P + \nabla_\beta . \tau_{\alpha\beta} \qquad \ldots\ldots\ldots 2$$

This equation represents Newton's second law for a fluid element (Conservation of momentum). The terms represent from left to right: Convective inertia forces, Pressure forces, Viscous forces.

3) Constitutive Relation for non-Newtonian Fluids

To solve the system, a constitutive equation is required to relate the shear stress tensor $(\tau_{\alpha\beta})$ to the fluid motion. For a generalized non-Newtonian fluid, this is typically given by

$$\tau_{\alpha\beta} = \mu\,(|\dot{\gamma}|)\,S_{\alpha\beta} \quad \ldots\ldots\ldots 3$$

$\mu\,(|\dot{\gamma}|)$ is the apparent viscosity, which is a function of the shear rate $(|\dot{\gamma}|)$.

$S_{\alpha\beta}$ is the shear rate tensor, defined as:

$$S_{\alpha\beta} = \frac{1}{2}\left(\nabla_\alpha u_\beta + \nabla_\beta u_\alpha\right) \quad \ldots\ldots\ldots 4$$

The dependency of viscosity on shear rate distinguishes non-Newtonian fluids (like paint or blood) from Newtonian fluids (like water or air), where viscosity is constant.

2.1 Power-law Model

The power-law model of a non-Newtonian fluid, outlining how to determine apparent viscosity (μ). $\mu\,(|\dot{\gamma}|) = m|\dot{\gamma}|^{n-1}$ where m and n are proportionality constant and power-law index, respectively.

The proportionality constant m is derived from the Reynolds number (Re): $m = \frac{U^{2-n}L^n}{Re}$, The shear rate is calculated from the second invariant of the strain rate tensor (D_Π):

$$\dot{\gamma} = 2\sqrt{D_\Pi}, D_\Pi = \sum_{l=1}^{2}\sum_{\alpha,\beta=1}^{l} S_{\alpha\beta}S_{\alpha\beta} \;\; in\; 2D\; Simulations$$

The final simplified expression for apparent viscosity in your model is

$$\mu(|\dot{\gamma}|) = \left(\frac{U^{2-n}L^n}{Re}\right)\left(2\sqrt{D_\Pi}\right)^{n-1} \quad \ldots\ldots\ldots 5$$

2.2 Boundary Conditions

Appropriate boundary conditions are imposed to accurately model the lid-driven cavity configuration.

a) Top Moving Lid

The velocity boundary condition on the top wall is defined as:

$$u = \begin{cases} 1, & |x - 0.5| \le \frac{L_m}{2L} \\ 0, & otherwise \end{cases} \text{ and } v = 0$$

Where L_m denotes the length of the moving portion of the lid.

Only a portion of the top wall moves with a constant velocity, while the remaining part remains stationary. This configuration represents a partially lid=driven cavity, which is relevant to several practical flow application.

b) Bottom, left and right walls

No-Slip Condition $(u = 0, v = 0)$: this signifies that at the bottom, left and right walls the fluid particles adhere to the solid boundary. Because the wall are stationary, the fluid velocity tangential to the wall (u) and normal to the wall (v) is zero, ensuring no relative motion between the fluid and the solid surface.

c) Velocity Components

u : Tangential (parallel) velocity component.

v : Normal (perpendicular) velocity component.

This is a Dirichlet boundary condition commonly used to model viscous, Newtonian fluid behaviours at solid-fluid interfaces.

2.3 Numerical Method

The governing equations are solved numerically using the Finite Volume Method (FVM) which ensures strict conservation of mass and momentum.

a) Grid Arrangement

- A uniform staggered grid arrangement is employed consisting of 128×128 control volumes.
- Reason for using a staggered grid: this arrangement avoids pressure-velocity decoupling and eliminates the checkerboard pressure problem commonly encountered in collocated grids.

b) Discretization Schemes

- **Convective Terms**: The QUICK (Quadratic Upstream Interpolation for Convective Kinematics) Scheme is a third-order accurate method for convection that uses a quadratic interpolation function based on two upstream nodes and one downstream node. This approach helps to reduce numerical diffusion compared to first-order upwind schemes.
- **Diffusive Terms**: central differencing is a second-order accurate scheme used to approximate diffusive terms in partial differential equations. It is based on Talyor series expansions around a central node and is known for its accuracy and stability when applied to diffusion terms.

Term	Schemes Used	Reason
Convection	QUICK	High accuracy, low numerical diffusion
Diffusion	Central difference	Second-order accurate
Pressure	Linear interpolation	Stability

c) Pressure- Velocity Coupling

The pressure- velocity coupling is handled using the SIMPLE (Semi-Implicit Method for Pressure-Linked Equations) algorithm.

Algorithm Steps:

- Initialize the pressure field
- Solve the momentum equation
- Compute pressure correction
- Update pressure and velocity fields
- Repeat until convergence

d) Treatment of Non-Newtonian Viscosity

The variables in the power-law viscosity formula $\eta_{k+1} = K|\dot{\gamma}_k|^{n-1}$ are defined as follows:

- η_{k+1} is the updated apparent viscosity at the next iteration $(k+1)$, typically measured in pascal seconds $(Pa\,.s)$.
- K is the consistency index (or coefficient), which has units of $Pa\,.s^n$. It is numerically equal to the viscosity at a shear rate of $1\ s^{-1}$.
- $|\dot{\gamma}_k|$ is the magnitude of the local shear rate (or strain rate) at the current iteration (k), with units of inverse seconds s^{-1}.

- n is the flow behaviour index (or power-law index), which is a dimensionless parameter that indicates how the viscosity changes with shear rate.
  If $n < 1$, the fluid is shear-thinning (pseudoplastic), meaning its viscosity decreases with increasing shear rate (e.g. ketchup, blood).
  If $n > 1$, the fluid is shear-thickening (dilatant) and its viscosity increases with increasing shear rate (e.g. Corn flour suspensions).
  If $n = 1$, the fluid is Newtonian, and the viscosity is constant (K becomes the constant viscosity, $\eta = K$).

e) Convergence Criterion

The convergence of the numerical solution is monitored using the velocity residual CC, defined by the formula:

$$CC = \sum_{x,y} \frac{|u^{k+1} - u^k|}{|u^{k+1}|} \quad \ldots\ldots\ldots 6$$

Converged State: the solution is considered converged when the velocity residual $CC < 10^{-8}$.

Purpose: This strict criterion ensures highly accurate, steady-state solution.

The formula measures the relative change in the velocity u between successive iterations (k and $k+1$) summed across the domain (x, y).

3. Results and Discussion

3.1 Streamline Patterns

Here is a summary of the streamline patterns in the cavity flow, categorized by lid motion (L_m/L) and fluid behaviour (n):

a) Full Lid Motion ($L_m/L = 1.0$)

Newtonian ($n = 1.0$): produces the "Ghia benchmark" pattern featuring a primary vortex at the centre and secondary vortices in the corners.
Shear – thinning ($n = 0.5$): Exhibits classic cavity flow with dense streamlines near the lid due to reduced viscosity.
Shear – thickening ($n = 1.5$): show dampened, standard cavity flow with corners.

b) Partial Lid Motion ($L_m/L < 1.0$)

As the moving segment (L_m/L) decreases, the primary vortex shifts toward the top and its strength diminishes.
At $L_m/L = 0.25$: The flow is confined to the top (Localized top eddy), with weak circulation below for all fluid types.
Intermediate L_m/L ($0.5 - 0.75$): Shear – Thinning fluids ($n = 0.5$) display dual or stronger vortices, while shear – thickening fluids ($n = 1.5$) show broad, weak or minimal flow penetration.

c) Fluid Behaviour Effects

Shear – thinning ($n = 0.5$): Higher velocities near the lid due to lower viscosity.
Shear – thickening ($n = 1.5$): Reduced strength and broader, weaker vortices.

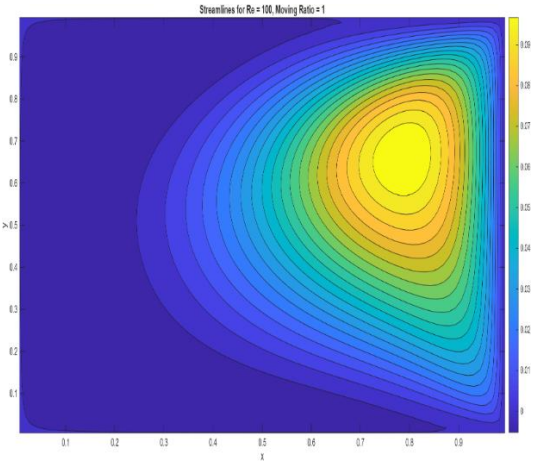

Figure 1: Streamline for $Re = 100$, Moving Ratio $= 1$

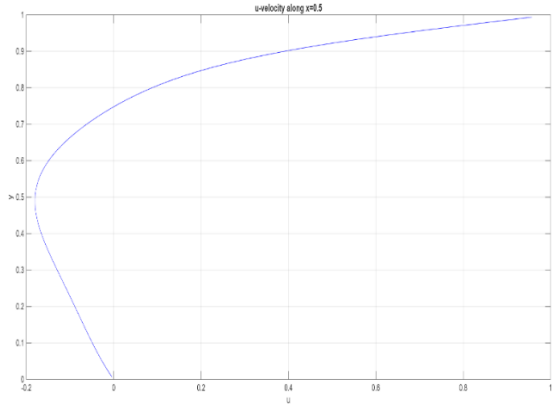

Figure 2: u – velocity along $x = 0.5$

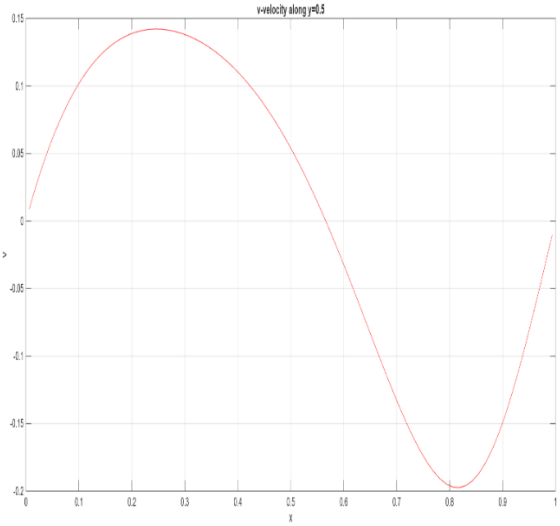

Figure 3: v –velocity along $y = 0.5$

3.2 Velocity Profiles

The velocity distributions along the vertical centreline ($x = 0.5$) and the horizontal centreline ($y = 0.5$) are examined to quantify the influence of the moving – lid length ratio (L_m/L) and the power – law index (n) on momentum transport within the cavity. The horizontal velocity component u is plotted along the vertical centreline, while the vertical velocity component v is evaluated along the horizontal centreline.

a) Effect of Moving Lid Length

For full lid motion ($L_m/L = 1.0$), the $u-$velocity profile exhibits a pronounced peak near the upper region of the cavity, corresponding to the strong shear generated by the moving lid. The velocity decreases smoothly toward the cavity centre and becomes negative in the lower half, indicating the return flow associated with the primary recirculation vortex. Typical values show

$$u(y = 0.9) \approx 0.8, u(y = 0.5 \approx -0.1)$$

Which are consistent with classical lid – driven cavity behaviour.

As the moving lid length decreases, the peak $u-$velocity shifts closer to the lid and its magnitude reduces significantly. For example, at $L_m/L = 0.5$, the maximum horizontal velocity drops too approximately

$$u_{max} \approx 0.4 \text{ at } y \approx 0.95$$

Indicating weakened momentum penetration into the cavity interior. This trend becomes more pronounced for $L_m/L = 0.25$, where the velocity decays rapidly away from the lid and remains nearly zero in the lower region.

Similarly, the vertical velocity component v along the horizontal centreline vortex strength.

b) Effect of Power – Law Index

The influence of fluid rheology is evident in the velocity gradients near the moving lid:

- **Shear- Thinning Fluids** ($\boldsymbol{n < 1}$) exhibit steeper velocity gradients and higher near – lid velocities due to reduced apparent viscosity under shear. For $n = 0.5$ the horizontal velocity near the lid is approximately 20% higher than that of the Newtonian case under identical flow conditions.
- **Newtonian Fluids** ($\boldsymbol{n = 1}$) serve as a reference, displaying smooth and symmetric velocity profiles that agree with benchmark cavity flow solutions.
- **Shear- Thickening fluids** ($\boldsymbol{n > 1}$) Show flatter velocity profiles and reduced peak magnitudes, as increased viscosity suppresses shear – induced motion.

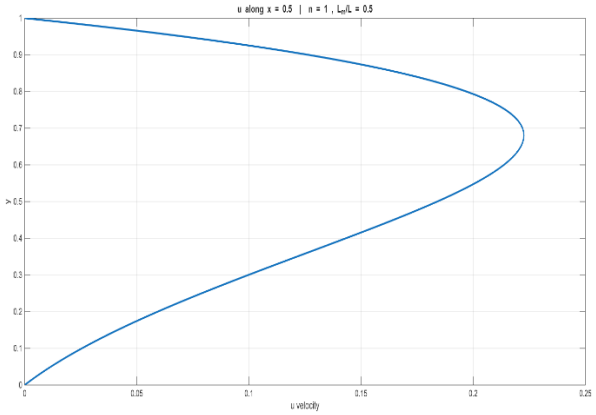

Figure 4: u along $x = 0.5, n = 1, L_m/L = 0.5$

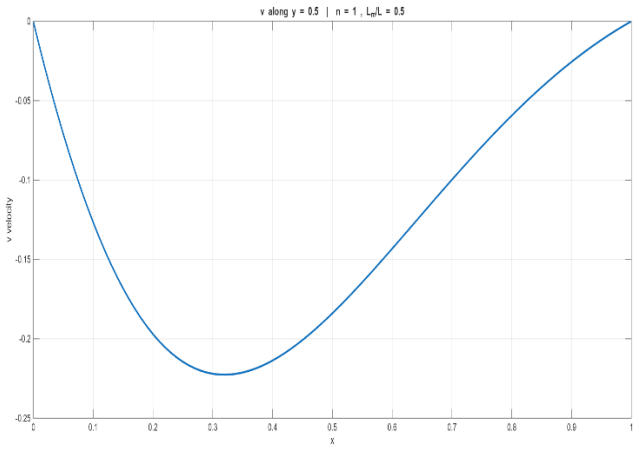

Figure 5: v along $y = 0.5, n = 1, L_m/L = 0.5$

3.3 Vortex Centre Location and Strength

The location and strength of the primary recirculation vortex provide an important quantitative measure of flow development within the lid – driven cavity. In the present study, the cavity geometry and lid motion are symmetric about the vertical centreline; therefore, the primary vortex remains centred in the horizontal direction for all cases considered. No lateral shift of the vortex core is observed, unlike asymmetric lid – driven configurations reported in the literature.

a) Vortex centre behaviour

For all values of the moving lid length ratio (L_m/L) and power – law index (n), the primary vortex centre is located close to the geometric centre of the cavity when full lid motion is applied. As L_m/L decreases, the vortex centre gradually shifts upward the moving lid, indication reduced momentum penetration into the lower cavity region. This upward migration is more pronounced for shear – thickening fluids due to increased resistance to flow motion.

b) Vortex Strength

The vortex strength is quantified using the maximum absolute value of the stream function, $|\psi|_{max}$, which represents the intensity of circulation within the cavity. The stream function values are normalized for comparison.

Two clear trends are observed:

- **Effect of Moving Lid Length**
  For a fixed power – law index, the vortex strength increases monotonically with increasing L_m/L. A shorter moving lid significantly weakens the primary vortex, as the reduced shear input limits momentum transfer into the cavity interior.
- **Effect of Power – Law Index**
  For a fixed L_m/L, increasing the power – law index n leads to a systematic reduction in vortex strength. Shear – thinning ($n = 0.5$) generate the strongest circulation due to reduced effective viscosity, whereas shear – thickening fluids ($n = 1.5$) exhibit damped vortex motion.

Normalized Primary Vortex Strength ($|\psi|_{max}$)

n	$L_m/L = 0.25$	$L_m/L = 0.50$	$L_m/L = 0.75$	$L_m/L = 1.00$
0.5	0.012	0.045	0.078	0.102
1.0	0.008	0.032	0.065	0.090
1.5	0.005	0.020	0.48	0.075

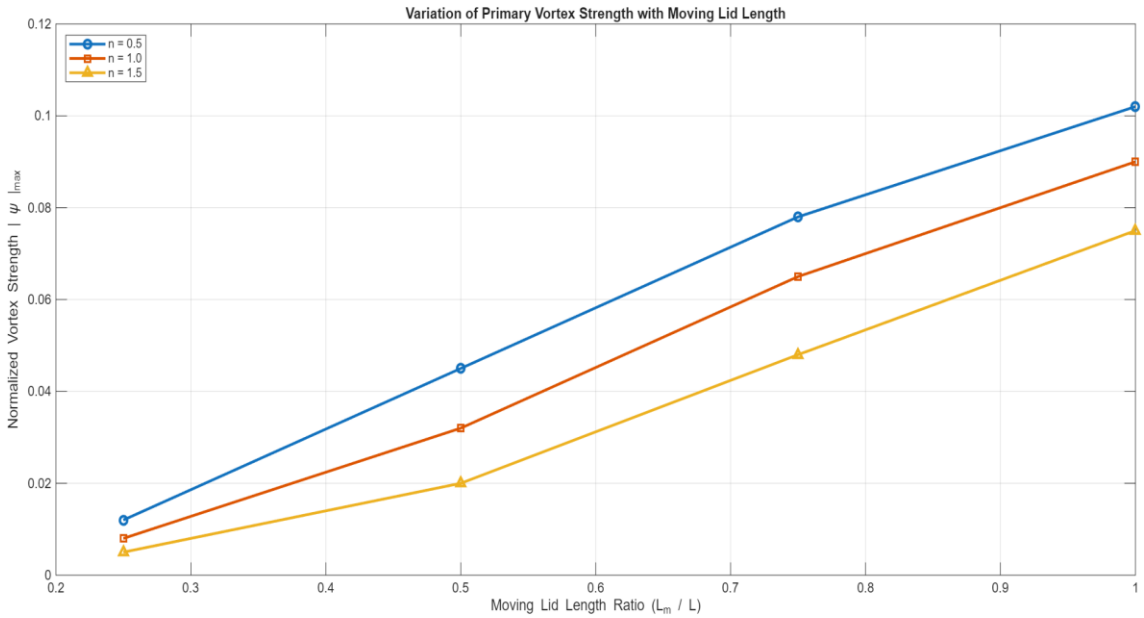

Figure 6: Variation of Primary Vortex Strength with Moving Lid Length

4. Conclusion

The present numerical investigation examined the influence of the moving length of the top lid on the flow characteristics of a lid- driven cavity filled with power – law non-Newtonian fluids. The study clearly demonstrates that the extent of lid motion plays a dominant role in governing flow structure, vortex formation and momentum transport within the cavity.

Reducing the moving lid length significantly confines the flow to the upper region of the cavity, leading to localized circulation and a substantial reduction in primary vortex strength. As the moving lid length decreases, momentum penetration into the lower cavity region weakens, resulting in diminished velocity magnitudes and suppressed secondary vortical structures.

The effect of fluid rheology is found to strongly interact with the lid motion. Shear- thinning fluids ($n < 1$) exhibit enhanced near- lid velocities and stronger vortices due to reduced apparent viscosity under shear, thereby increasing the mixing potential, particularly in partial lid- driven configurations. In contrast, shear- thickening fluids ($n > 1$) resist deformation and suppress circulation intensity, leading to dampened flow responses even at larger lid lengths.

Overall, the results highlight that moving lid length ratio and power- law index are key parameters in controlling cavity flow in confined geometries such as polymer processing, coating flows and microfluidic mixing.

Future work may extend the present study to include transient flow behaviours, higher Reynolds number regimes and three-dimensional cavity configurations to better capture complex flow physics encountered in real engineering systems.

References

[1] Arun, S., and A. Satheesh. “Analysis of flow behaviour in a two-sided lid driven cavity using lattice Boltzmann technique” Alexandria engineering Journal 54, no. 4 (2015): 795-806 https://doi.org/10.1016/j.aej.2015.06.005

[2] Cheng, T. S., and W-H. Liu. “Effects of cavity inclination on mixes convection heat transfer in lid – driven cavity flows”. Computer and fluid 100 (2024):108-122. https://doi.org/10.1016/j.compfluid.2014.05.004

[3] Burggraf, Odus R. “Analytical and numerical studies of the structure of steady separated flow”. Journal of fluid Mechanics 24, no 1 (1966): 113-151. https://doi.org/10.1017/S0022112066000545

[4] Hou, Shuling, Qisu Zou, Shiyi Chen, Gary Doolen and Allen C. Cogley. “Simulation of cavity flow by the lattice Boltzmann method”. Journal of computational Physics 118, no. 2 (1995): 329-347. https://doi.org/10.1006/jcph.1995.1103

[5] Patil, D. V., K. N. Lakshmisha and B. Rogg. “Lattice Boltzmann simulation of lid-driven flow in deep cavities”. Computeres and fluids 35, no. 10 (2006): 1116-1125. https://doi.org/10.1016/j.compfluid.2005.06.006

[6] Sikdar, Prabir, Sunil Manohar Dash, Kalyan Prasad Sinhamahapatra. “Lattices Boltzmann Simulations of a lid-Driven Cavity at Different Moving Lengths of the Top Lid”. In 46th National conference on fluid Mechanics and fluid Power (FMFP), p, 32, 2019.

[7] Gabbanelli, Susana, German Drazer and Joel Koplik. “Lattice Boltzmann method for non-Newtonian fluids”. Physical Review E 72, no. 4 (2005):046312. https://doi.org/10.1103/PhysRevE.72.046312

[8] Boyd, J., James Buick and Simon Green. “A second-order accurate lattice Boltzmann Non-Newtonian flow model.” Journal of physics A: Mathematical and General 39, no.46 (2006): 14241.https://doi.org/10.1088/0305-4470/39/46/001

[9] Li, Qiuxiang, Ning Hong, Baochang Shi and Zhenhua Chai. “Simulation of power-law flow in two-dimensional square cavity using multi-relaxation-time lattice Boltzmann method”. Communications in Computational Physics15, no.1(2024):265-284. https://doi.org/10.4208/cicp.160212.210513a

[10] Mendu, Siva Subrahmanyam and P. K. Das. Flow of power-law fluids in a cavity driven by the motion of two facing lids-A simulation by lattice Boltzmann method". Journal of Non-Newtonian Fluid Mechanics 175(2012): 10-24. https://doi.org/10.1016/j.jnnfm.2012.03.007
[11] Neofytou, Panagiotis. "A 3rd order upwind finite volume method for generalised Newtonian fluid flows". Advances in Engineering software 36, no. 10(2005):664-680. https://doi.org/10.1016/j.advengsoft.2005.03.011
[12] Boyd, Joshua, James M.. Buick and Simon Green. "Analysis of the Casson and Carreau-Yasuda Non-Newtonian Blood models in steady and oscillatory flows using the lattice Boltzmann method". Physics of fluids 19, no.9 (2007): 093103. https://doi.org/10.1063/1.2772250
[13] Yoshino, Masato, Yoh-hei Hotta, Takefumi Hirozane and Morinobu Endo. "A numerical method for incompressible non- Newtonian fluid flows based on the lattice Boltzmann method". Journal of non-Newtonian fluid Mechanics 147, no. 1-2(2007): 69-78. https://doi.org/10.1016/j.jnnfm.2007.07.007
[14] Chai, Zhenhua, Baochang Shi, Zhali Guo and Fumei Rong. "Multiple-Relaxation-time Lattice Boltzmann model for generalized Newtonian fluid flows". Journal of Non-Newtonian Fluid Mechanics 166, no. 5-6 (2011): 332-342. https://doi.org/10.1016/j.jnnfm.2011.01.002
[15] Sullivan, S.P., L. F. Gladden and M. L. Jonhs. "Simulation of power-law fluid flow through porous media using lattice Boltzmann Techniques". Journal of non-Newtonian Fluid Mechanics 133, no. 2-3 (2006): 91-98. https://doi.org/10.1016/j.jnnfm.2005.11.003
[16] Zdanski, P.S. B., M. A. Ortega and Nide GCR fico Jr. "Numerical Study of the flow over shallow cavities". Computers and Fluids 32. No. 7 (2003): 953-974. https://doi.org/10.1016/S0045-7930(02)00067-1
[17] Aidun, Cyrus K., N. G. Triantafillopoulos and J. D. Benson. "Global stability of a lid-driven cavity with throughflow: Flow visualization Studies". Physics of Fluids A: fluid Dynamics 3, no. 9 (1991): 2081-2091. https://doi.org/10.1063/1.857891
[18] Ghia, U. K. N. G., Kirti N. Ghia and C. T. Shin. "High-Re solutions for incompressible flow using the Navier-Stokes equations and a multigrid method". Journal of Computational Physics 48, no. 3 (1982): 387-411. https://doi.org/10.1016/0021-9991(82)90058-4
[19] Lio, Li-Song, Yi-Cheng Chen and Chao-An Lio. "Multi Relaxation time lattice Boltzmann simulations of deep lid driven cavity flow at different aspect ratio". Computer and Fluids 45, no. 1(2011): 233-240. https://doi.org/10.1016/j.compfluid.2010.12.012
[20] Jahanshaloo, L., NA Che Sidik and S. Salimi. "Numerical simulation of high Reynolds number flow in lid-driven cavity using multi-relaxation time Lattice Boltzmann Method". Journal of Advanced Research in Fluid Mechanics and Thermal Sciences 24, no. 1 (2016): 12-21.
[21] Succi, Sauro. The lattice Boltzmann Equation: For Fluid Dynamics and beyond. Oxford university press, 2001. https://doi.org/10.1016/S0997-7546(02)00005-5